DOI: 10.18721/JPM.10403
UDC 536.24.08

IMPACT OF NANOPARTICLE VOLUME FRACTIONS IN THE WATER-BASED NANOFLUIDS ON THE SQUEEZED MHD NANOFLUID'S FLOW OVER A POROUS SENSOR SURFACE

R. Kandasamy, N.A.B.M. Zailani, F.N.B.J. Fatiha

Research Centre for Computational Mathematics,
Tun Hussein Onn University of Malaysia, Parit Raja, Malaysia

The squeezed MHD flow of water-based metallic nanoparticles over a porous sensor surface in the presence of a heat source has been investigated. The physical significance of the problem is the interaction and the geometry of water-based copper (Cu), alumina (Al_2O_3) and SWCNTs. The governing partial differential equations of momentum and energy were converted into ODEs for assured groups of the controlling parameters. The numerical and analytical solutions of the ODEs were obtained using the fourth or the fifth order Fehlberg method with shooting technique and OHAM and were analyzed. It was found that there was no appreciable difference between them. It was established that, in squeezing flow phenomena, the effect of nanoparticle volume fraction on the (SWCNTs − water) nanofluid in the presence of magnetic field with thermal radiation energy played a dominant role on heat transfer as compared to the other mixtures in the flow regime.

Keywords: nanoparticle volume fraction; squeezed flow; sensor surface; SWCNT; thermal radiation energy

Citation: R. Kandasamy, N.A.B.M. Zailani, F.N.B.J. Fatiha, Impact of nanoparticle volume fractions in the water-based nanofluids on the squeezed MHD nanofluid's flow over a porous sensor surface, St. Petersburg Polytechnical State University Journal. Physics and Mathematics. 10 (4) (2017) 34–53. DOI: 10.18721/JPM.10403

ВЛИЯНИЕ ОБЪЕМНЫХ ДОЛЕЙ НАНОЧАСТИЦ В ВОДНЫХ НАНОЖИДКОСТЯХ НА ХАРАКТЕРИСТИКИ СЖИМАЕМОГО МГД-ПОТОКА ЭТИХ ЖИДКОСТЕЙ ПО ПОРИСТОЙ ПОВЕРХНОСТИ ДАТЧИКА

Р. Кандасами, Н.А.Б.М. Зайлани, Ф.Н.Б.Дж. Фатиха

Исследовательский центр вычислительной математики
Малайзийского университета Туна Хусейна Онна, г. Парит Раджа, Малайзия

Исследованы сжимаемые магнитогидродинамические (МГД) потоки наножидкостей (вода + наночастицы трех типов) по поверхности пористого чувствительного элемента в присутствии теплового источника. Физическая суть задачи состоит в получении профилей основных характеристик потоков при воздействии указанных факторов и в анализе взаимодействия с водой наночастиц меди (Cu), глинозема (Al_2O_3) и одностенных углеродных нанотрубок (ОУНТ). Определяющие дифференциальные уравнения с частными производными относительно импульса и энергии были преобразованы в обыкновенные дифференциальные уравнения (ОДУ) относительно гарантированных групп управляющих параметров. Численные и аналитические решения ОДУ найдены с применением метода Фельберга 4-го и 5-го порядков с математическим

пристреливанием и асимптотического метода оптимальных гомотопий. Анализ показал, что между численными и аналитическими решениями нет значимой разницы. Установлено, что в явлениях сжатия потока доминирующую роль играет объемная доля наночастиц. Система вода – ОУНТ показала наилучшие характеристики теплопереноса в режиме течения под действием магнитного поля и теплового излучения, по сравнению с другими системами.

Ключевые слова: объемная доля наночастиц; сжимаемый поток; поверхность датчика; ОУНТ; энергия теплового излучения

Ссылка при цитировании: Кандасами Р., Зайлани Н.А.Б.М., Фатиха Ф.Н.Б.Дж. Влияние объемных долей наночастиц в водных наножидкостях на характеристики сжимаемого МГД-потока этих жидкостей по пористой поверхности датчика // Научно-технические ведомости СПбГПУ. Физико-математические науки. 2017. Т. 10. № 4. С. 34–53. DOI: 10.18721/JPM.10403

Introduction

Nanofluids are conceivable thermal energy transfer fluids with uprated thermophysical properties and heat-transfer performance; they can be activated in many devices for better enforcement (i.e., energy, heat-transfer and other performances). In nanotechnology, a particle is defined as a small localized object of substance that reacts as a perfect unit with regard to its transport and resources. Particles are limited on the sizes. Nanoparticle research is currently an area of great scientific importance due to an extensive cast of possible operations in medical, optical and electrical fields. Squeezed flow within parallel walls has attracted the attention of more and more researchers in the field of mechanics. The interest in this phenomenon is due to its potential for use in engineering, fluid metal purification, foodstuff and chemical industries, compression and injection shaping, etc. In addition to an academic interest, squeezing nanofluid flow presents a range of applications at the industry level such as petroleum, biochemical technology, foodstuff engineering and medicine manufacturing [1 – 5]. The effect of the magnetic field normal to the flow of thermally conducting nanofluid on the boundary layer over a flat wall is extensively discussed in the literature [6 – 7]. Recently, the effects of magnetic strength on oscillatory squeezed discharges have been analyzed inside thin films by Khaled and Vafai [8] where they have established that magnetic strength can decrease a recurving ability inside thin films correlated with immense squeezing issues. In any case, the literature lacks reviews about the issues of magnetic range in flow and, correspondingly, on thermal and diffusion transfer past a sensor wall located within fluidic cells, with account of squeezed flow conditions. The conventional heat transfer nanofluids, including oil, ethylene glycol and water have weak thermal energy conductivity compared to solids. To increase the thermal energy conductivity of these fluids, small particles (nanoparticles) of the solids possessing stronger thermal energy conductivity are integrated within the base fluid which provides a better heat transfer rate [9 – 19].

Nanofluid, i.e., an admixture of nanoparticles and water, is a new type of energy transport fluid. The fluids with remarkably enhanced thermal energy conductivity have been useful for several engineering and industrial purposes. Cooling rate necessities may not be achieved by the use of ordinary heat transfer fluids since these fluids show reduced thermal energy conductivity. Thermal conductivity and thermal performance of ordinary heat transfer fluids may be increased by immersing the nanoparticles. Novel properties of nanofluids make them potentially applicable as a distinct mechanism of thermal energy transfer in digital electronics, fuel cells, hybrid-powered engines, etc. It is hoped that MHD investigation of nanofluids is important in optical gratings, optical switches, ink float partition, cancer therapy by piloting active particles in the bloodstream to a tumor with magnets. Masuda et al. [20] studied the alterations in heat conductivities and viscosities of liquids through the dispersion of ultrafine particles in the base fluids. Choi [21] found that the presence of nanoparticles in the base fluid enhances the thermal properties of fluids.

The strengthening of heating in an industrial process may create a decrease in energy and growth time, increase in heat rating and

prolong the working life of equipment. Some processes are even affected qualitatively by the action of increased thermal energy transfer. The development of high-performance thermal systems for heat transfer enrichment has become attractive nowadays. A number of studies have been performed to gain an understanding of thermal energy transfer enforcement for experimental application to heat transfer enhancement. Thus, the advent of high heat flow development has generated sufficient appeal for new researches to enhance heat transfer. Single-walled carbon nanotubes (SWCNTs), a member of the carbon family, are one-dimensional equivalents of zero-dimensional decomposed molecules with rare constitutional and electronic properties. Single-walled nanotubes are the most likely candidate for miniaturizing electronics beyond the micro electro-thermal scale presently utilized in electronics. Carbon nanotubes (CNTs) have been the focus of much attention because of their linear model and notable mechanical, thermal, and electrical properties [22 – 26]. CNTs have been used as preservatives in liquids to enhance thermal energy conductivity, one of the most important issues in industry. Applications of nanofluids in industries such as heat exchanging devices appear promising with these properties. Anyway, the improvement and applications of nanofluids may be hindered by several factors such as enhanced pushing power and pressure drop, nanofluids' thermal performance in turbulent flow, lesser specific heat of nanofluids and higher production cost of nanofluids.

The object of the present work is to analyze the effects of nanoparticle volume fraction on copper, aluminum and CNTs suspended in water-based unsteady external squeezing MHD flow over a flat permeable sensor wall in the existence of thermal radiation energy.

The analysis is concerned with a certain group of squeezed flows such that the occurring flows may be solved using similarity transformations and afterwards the problem is analyzed by applying the fourth or fifth order Fehlberg technique with the shooting method and OHAM. Several aspects of the problem are investigated and presented graphically taking into account the physical parameters involved within it and the results obtained are correlated with the applicable literature.

Mathematical analysis

In this study, an unsteady two-dimensional MHD squeezing nanofluid flow being between two infinite parallel plates is considered. Natural flow composition of this problem is given in such a way that the plate is enclosed inside a squeezed channel so that the height $h(t)$ is more than the boundary layer thickness and the squeezing in the free stream is expected to exit from the edge of the wall (Fig. 1). A microcantilever sensor is placed within the walls and the upper wall is compressed while lower plate being fixed. The working nanofluid is assumed to be Newtonian and electrically conducting with σ as its electrical conductance and the magnetic field with a time-dependent strength B_0 is stimulated perpendicular to the flow in the y-direction while the induced magnetic Reynolds number is negligible. The system of controlling equations is defined [27, 28, 32] as

$$\frac{\partial u}{\partial x}+\frac{\partial v}{\partial y}=0, \tag{1}$$

$$\frac{\partial u}{\partial t}+u\frac{\partial u}{\partial x}+v\frac{\partial u}{\partial y}= \tag{2}$$

$$=-\frac{1}{\rho_{nf}}\left(\frac{\partial p}{\partial x}\right)+\nu_{nf}\left(\frac{\partial^2 u}{\partial y^2}\right)-\left(\frac{\mu_{nf}}{\rho_{nf}K}+\frac{\sigma_{nf}B_0^2}{\rho_{nf}}\right)u,$$

$$\frac{\partial U}{\partial t}+U\frac{\partial U}{\partial x}=-\frac{1}{\rho_{nf}}\left(\frac{\partial p}{\partial x}\right)-\frac{\sigma_{nf}B_0^2}{\rho_{nf}}U, \tag{3}$$

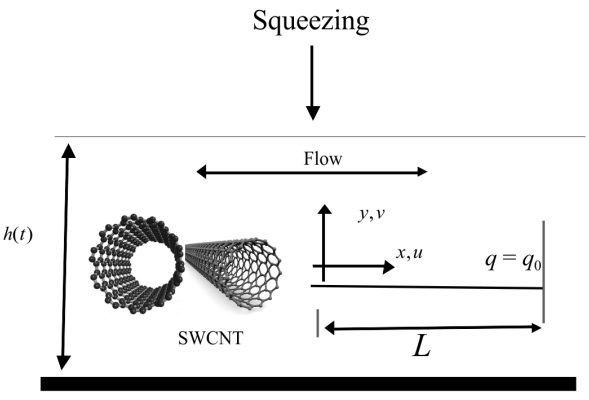

Fig. 1. Flow configuration and coordinate system

$$\frac{\partial T}{\partial t} + u\frac{\partial T}{\partial x} + v\frac{\partial T}{\partial y} = \\ = \alpha_{nf}\frac{\partial^2 T}{\partial y^2} - \frac{1}{(\rho\, c_p)_{nf}}\frac{\partial q_r}{\partial y} + \frac{Q_0(T - T_\infty)}{(\rho\, c_p)_{nf}}. \quad (4)$$

with boundary conditions

$$u(x,0,t) = 0,\ v(x,0,t) = v_0(t), \\ -k_{nf}\frac{\partial T(x,0,t)}{\partial t} = q(x), \quad (5) \\ u(x,\infty,t) = U(x,t), T(x,\infty,t) = T_\infty,$$

where u, v are the velocity components in the x and y directions; T is the temperature of the nanofluid; t is the time; p is the fluid pressure; σ_s, σ_f are the electrical conductivity of the base fluid and the nanofluid; v_0 is a constant; U is the free-stream velocity; a is a constant; Q_0 is the heat generation or absorption coefficient.

Physically, $v_w < 0$ means injection, and $v_w > 0$ implies suction of fluid; the magnetic Reynolds number is considered so small that the magnetic boundary-layer thickness is extensive and the convenient magnetic field is gradual compared with the applied magnetic field. For particle-fluid mixtures, several theoretical studies have been carried out starting with Maxwell's classical works [29, 30]. The Maxwell structure for thermal energy conductivity for solid – liquid combining relatively large particles (micro-/mini- size) is good for fine solid species. Viscosity reflects a fluid's internal resistance to flow and, in the case of nanofluids, depends on the nature and a size of particles. The thermophysical properties established in the nanofluid are defined as

$$\alpha_{nf} = \frac{k_{nf}}{(\rho\, c_p)_{nf}},\ \rho_{nf} = (1-\zeta)\rho_f + \zeta\rho_s, \\ \mu_{nf} = \frac{\mu_f}{(1-\zeta)^{2,5}}, \\ (\rho\, c_p)_{nf} = (1-\zeta)(\rho\, c_p)_f + \zeta(\rho\, c_p)_s, \quad (6) \\ \sigma_{nf} = (1-\zeta)\sigma_f + \zeta\sigma_s, \\ \frac{k_{nf}}{k_f} = \left\{\frac{(k_s + 2k_f) - 2\zeta(k_f - k_s)}{(k_s + 2k_f) + 2\zeta(k_f - k_s)}\right\}.$$

where ζ is the nanoparticle volume fraction; μ_f is the dynamic viscosity of the basic fluid; β_f, β_s are the volumetric extension coefficients of the water and nanoparticle, respectively; ρ_f, ρ_s are the densities of the basic fluid and nanoparticle; σ_f, σ_s are the electric conductivities of the basic fluid and nanoparticle; k_f is the thermal conductivity of the fluid; k_s is the thermal energy dynamism of the solid fraction.

Let us employ Rosseland's approximation [31]:

$$q''_{rad} = q_r = -\frac{4\sigma_1}{3k^*}\frac{\partial T^4}{\partial y},$$

where σ_1 is the Boltzmann constant, k^* is the penetration coefficient.

Expanding Taylor's series with T^4 being

$$T^4 \cong 4T_\infty^3 T - 3T_\infty^4,$$

we obtain

$$\frac{\partial q_r}{\partial y} = -\frac{16\sigma_1 T_\infty^3}{3k^*}\frac{\partial^2 T}{\partial y^2}.$$

Based on the free-stream condition, Eqs. (2), (3) become

$$\frac{\partial u}{\partial t} + u\frac{\partial u}{\partial x} + v\frac{\partial u}{\partial y} = \frac{\partial U}{\partial t} + U\frac{\partial U}{\partial x} + \frac{\mu_{nf}}{\rho_{nf}}\frac{\partial^2 u}{\partial y^2} - \\ -\left(\frac{\mu_{nf}}{\rho_{nf}K_0} + \frac{\sigma_{nf}B_0^2}{\rho_{nf}}\right)(u - U), \quad (7)$$

where

$$U\frac{dU}{dx} = -\frac{1}{\rho_{nf}}\frac{\partial P}{\partial x} - \left(\frac{\mu_{nf}}{\rho_{nf}K_0} + \frac{\sigma_{nf}B_0^2}{\rho_{nf}}\right)U;$$

K_0 is the nonuniform permeability of the medium; B_0 is the externally imposed magnetic strength in the y-direction.

The stream function can be obtained from Eq. (1) as

$$u = \frac{\partial\psi}{\partial y},\ v = -\frac{\partial\psi}{\partial x}. \quad (8)$$

Based on Eq. (8) with the similarity variables, we have

$$\eta = y\sqrt{\frac{a}{\nu_f}},\ \psi = \sqrt{a\nu_f}\, xf(\eta), a = \frac{1}{s+bt}, \\ \theta(\eta) = \frac{T - T_\infty}{\frac{q_0 x}{k_f}\sqrt{\frac{\nu_f}{a}}},\ q(x) = q_0 x, v_0(t) = v_i(t), \quad (9)$$

where b, s are random constants; a is the strength of squeezing flow; q_0 is the heat flux; v_0 is the velocity on the sensor surface when permeable walls are designed.

Taking into account the conditions given by Eq. (9), the dynamics of the channel's height governs by the following conditions:

$$h(t) = h_0 / (s + bt)^{-\frac{1}{b}} \text{ for } b > 0;$$

$$h(t) = h_0 e^{-st} \text{ for } b = 0.$$

The surface permeable velocity is established to increase as the time decelerates ($b > 0$) because compressing velocities enhance as time decelerates.

Eqs. (4) and (7) become

$$f''' + A_1\left(\left(f + \frac{b\eta}{2}\right)f'' - f'^2 + b(f'^2 - 1) + \right. \\ \left. + \left(M\frac{A_2}{A_1} + \frac{\lambda}{A_1}\right)(1 - f') + 1\right) = 0. \quad (10)$$

$$\frac{1}{\Pr}\left(\frac{k_{nf}}{k_f A_3} + \frac{\Pr R}{k_f A_3}\right)\theta'' + \\ + \left(\frac{\delta}{A_3}\theta + \left(f + \frac{b\eta}{2}\right)\theta' - \left(f' + \frac{b}{2}\right)\theta\right) = 0. \quad (11)$$

with boundary conditions

$$f(0) = S, f'(0) = 0, \theta'(0) = -\frac{k_f}{k_{nf}}; \\ f'(\infty) \to 1, \theta(\infty) \to 0, \quad (12)$$

$$A_1 = (1 - \zeta)^{2,5}\left(1 - \zeta + \zeta\frac{\rho_s}{\rho_f}\right),$$

$$A_2 = (1 - \zeta)^{2,5}\left(1 - \zeta + \zeta\frac{\sigma_s}{\sigma_f}\right), \quad (13)$$

$$A_3 = \left(1 - \zeta + \zeta\frac{(\rho c_p)_s}{(\rho c_p)_f}\right),$$

where $\Pr = (c_p\mu)_f / k_f$ is the Prandtl number;

$$\delta = \frac{Q_0 x}{(\rho c_p)_f U}$$

is the heat source/sink parameter;

$$\lambda = \frac{\nu_f x}{UK}$$

is the porous parameter;

$$M = \frac{\sigma_f B_0^2 x}{U\rho_f}$$

is the magnetic parameter;

$$R = \frac{16\sigma_1\theta_w^3}{3k_f k^*}$$

is the thermal energy radiation parameter.

The physical quantities are as follows:

$$C_f = \frac{\tau_w}{\rho_f U^2}$$

is the skin friction coefficient;

$$\mathrm{Nu}_x = \frac{q_w x}{k_f(T_w - T_\infty)}$$

is the local Nusselt number (τ_w and q_w are defined as

$$C_f(\mathrm{Re}_x)^{1/2} = \frac{f''(0)}{(1 - \zeta)^{2,5}}, \frac{\mathrm{Nu}_x}{\mathrm{Re}_x^{1/2}} = -\frac{k_{nf}}{k_f}\theta'(0)); \quad (14)$$

$\mathrm{Re}_x = \frac{Ux}{\nu_f}$ is the local Reynolds number.

Results and discussion

Computations were worked out using the OHAM (Optimal Homotopy Asymptotic Method) and the fourth or fifth order Fehlberg technique with the shooting approach (numerical mechanism) for various values of the parameters. Eqs. (10) and (11) subjected to boundary conditions (12) were determined numerically and experimentally utilizing the Maple 18 and Mathematica 5.2 computer software. We have completely simulated the described processes.

Thermophysical properties of the fluid and the nanoparticles are given in Table 1.

The Prandtl number Pr = 6.2 corresponds to nanofluids unless otherwise specified. In order to validate our methods, it is predicted from Fig. 2 that the consistency with the theoretical solution of the temperature profiles and $f''(0)$ for various character of ζ are correlated with the results presented in Fig. 4, *b* and Table 2 (water-based Cu and Al_2O_3 when $\zeta = 0.0$) of Ref. [32]. Excellent agreement can be observed between them.

Table 1

Thermophysical properties of the fluid and the nanoparticles

Substance	ρ, kg/m^3	c_p, J/(kg·K)	k, W/(m·K)
Pure water	997.1	4179	0.613
Copper (Cu)	8933	385	401
Aluminum (Al_2O_3)	3970	765	40
SWCNTs	2600	425	6600

Notations: ρ is the density, c_p is the specific heat at the constant pressure, k is the thermal conductivity coefficient; SWCNTs are Single-Walled Carbon NanoTubes.

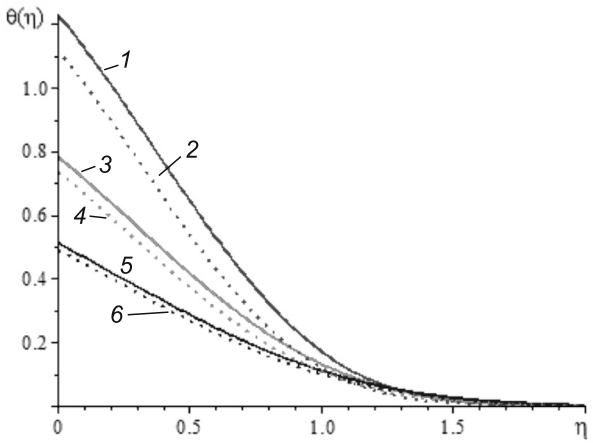

Fig. 2. Temperature profiles for (Cu − water) nanofluid flow for various nanoparticle volume fractions ζ and two M values;
ζ = 0.0 (curves *1*, *2*), 0.1 (*3*, *4*), 0.2 (*5*, *6*); M = 0.0 (*1*, *3*, *5*) and 1.0 (*2*, *4*, *6*).
Comparison to Fig. 4, *b* of Ref. [32]

Table 2

Comparison of impacts of nanoparticle volume fraction ζ on $f''(0)$

Nanofluid	ζ value	$f''(0)$		Error between two methods
		Numerical method	OHAM	
Cu − water	0.0	1.48113419 [32]	1.48113419 [32]	0.00000000
	0.1	1.71105504	1.71105531	2.7E − 07
	0.2	1.75138728	1.75138766	3.8E − 07
Al_2O_3 − water	0.0	1.48113419 [32]	1.48113419 [32]	0.00000000
	0.1	1.43438455	1.43438501	4.6E − 07
	0.2	1.33096758	1.33096794	3.6E − 07
SWCNTs − water	0.0	1.48113419 [32]	1.48113419 [32]	0.00000000
	0.1	1.45088235	1.45088232	3.0E − 08
	0.2	1.35571879	1.35571877	2.0E − 08

OHAM is the Optimal Homotopy Asymptotic Method

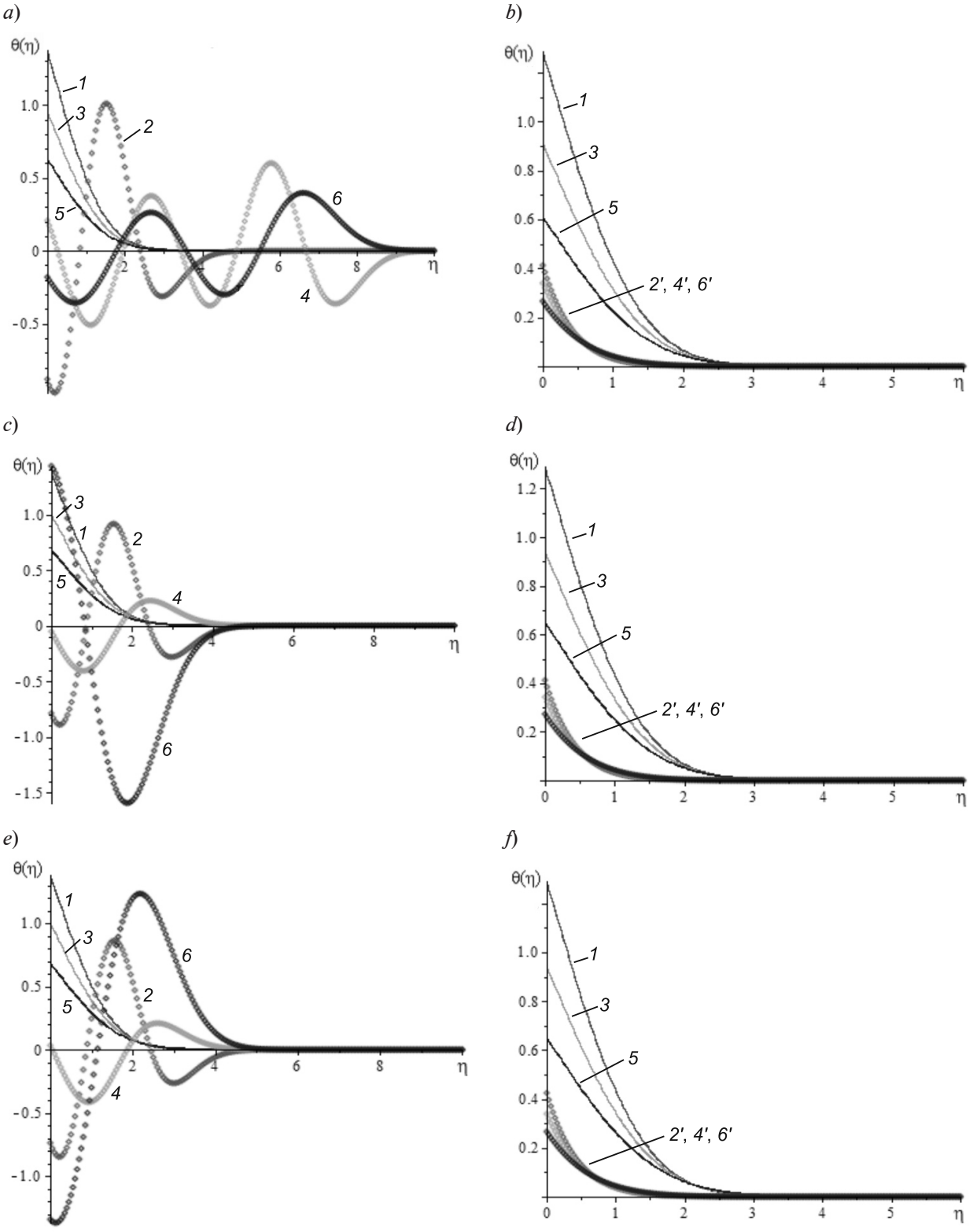

Fig. 3. Temperature profiles for flows of 3 nanofluid's compositions with various nanoparticle volume fractions ζ and three δ values, in the presence of heat source (*a*, *c*, *e*) and heat sink (*b*, *d*, *f*); there are (Cu − water) (*a*, *b*), (Al_2O_3 − water) (*c*, *d*) and (SWCNTs − water) (*e*, *f*) nanofluids;
ζ = 0.01 (curves *1*, *2*, *2′*), 0.1 (*3*, *4*, *4′*), 0.2 (*5*, *6*, *6′*); δ = 0.0 (*1*, *3*, *5*), 1.0 (*2*, *4*, *6*), −1.0 (*2′*, *4′*, *6′*)

Table 3

Values of θ' (0) for various values of ζ and δ obtained for different nanofluids

δ	ζ	θ' (0)		
		Cu−water	Al_2O_3−water	SWCNTs−water
−1.0	0.01	0.4120137	0.4124028	0.4242504
	0.10	0.3393746	0.3429119	0.3391175
	0.20	0.2662112	0.2729732	0.2665138
0.0	0.01	1.3756611	1.3756611	1.3844948
	0.10	0.9537223	0.9981022	1.0019741
	0.20	0.6317888	0.6845075	0.6872416
1.0	0.01	−0.8804759	−0.7885852	−0.73798356
	0.10	0.2069197	−0.0527793	0.0342681
	0.20	−0.1802860	1.4355837	−1.3426626

Fixed parameter values: Pr = 6.2, S = 0.5, b = 0.5, M = 1.0, R = 1.0.

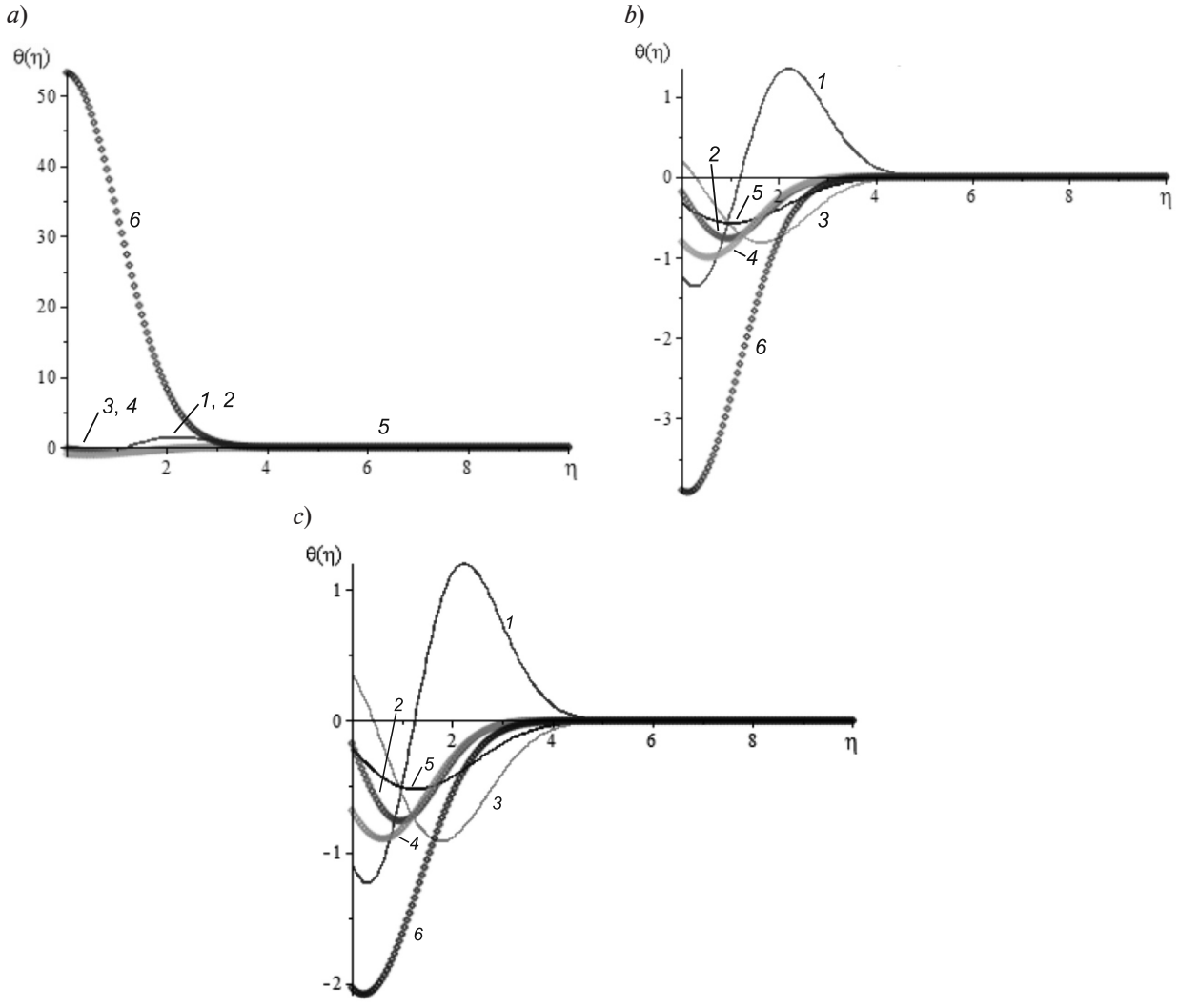

Fig. 4. Temperature profiles for flows of 3 nanofluid's compositions with various nanoparticle volume fractions ζ and two b values, in the presence of squeezed flow; there are (Cu − water) (*a*), (Al_2O_3 − water) (*b*) and (SWCNTs − water) (*c*) nanofluids;
ζ = 0.01 (curves *1*, *2*), 0.1 (*3*, *4*), 0.2 (*5*, *6*); b = 0.0 (*1*, *3*, *5*) and 1.0 (*2*, *4*, *6*)

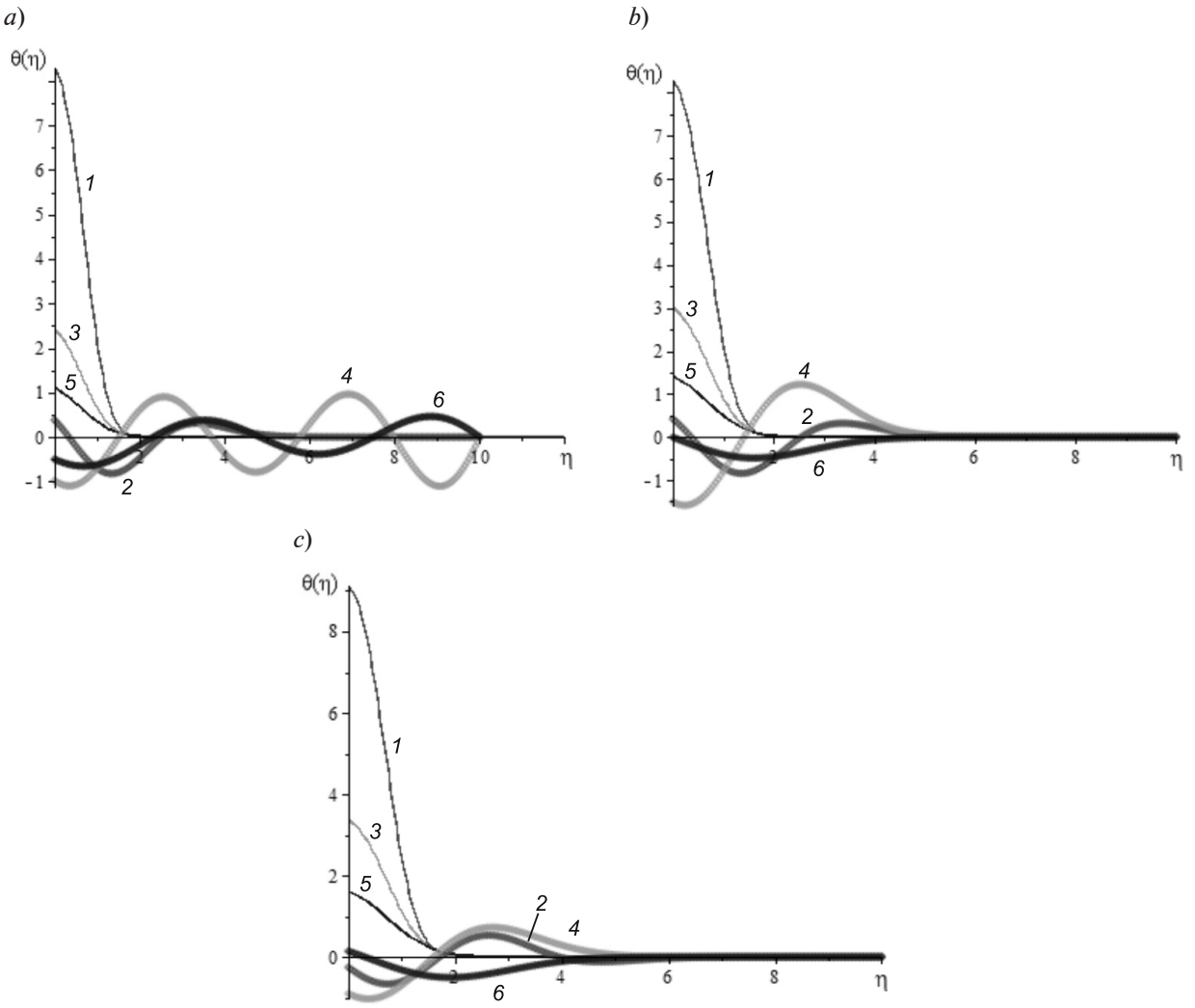

Fig. 5. Temperature profiles for flows of 3 nanofluid's compositions with various nanoparticle volume fractions ζ and two R values, in the presence of thermal radiation; there are (Cu − water) (*a*), (Al_2O_3 − water) (*b*) and (SWCNTs − water) (*c*) nanofluids;
ζ = 0.01 (curves *1*, *2*), 0.1 (*3*, *4*), 0.2 (*5*, *6*); R = 0.0 (*1*, *3*, *5*) and 1.0 (*2*, *4*, *6*)

Table 4

Values of θ' (0) for various values of ζ and R obtained for different nanofluids

R	ζ	θ' (0)		
		Cu−water	Al_2O_3−water	SWCNTs−water
−1.0	0.01	8.2923900	8.2923900	9.1264301
	0.10	2.4082687	3.0094599	3.3680544
	0.20	1.1025964	1.4040971	1.6065768
1.0	0.01	0.3819982	0.4199881	−0.2552729
	0.10	−0.9759417	−1.5083132	0.1398253
	0.20	−0.4970868	−0.0074834	0.1398253

Fixed parameter values: Pr = 6.2, S = 0.5, b = 0.5, M = 1.0, δ = 1.0.

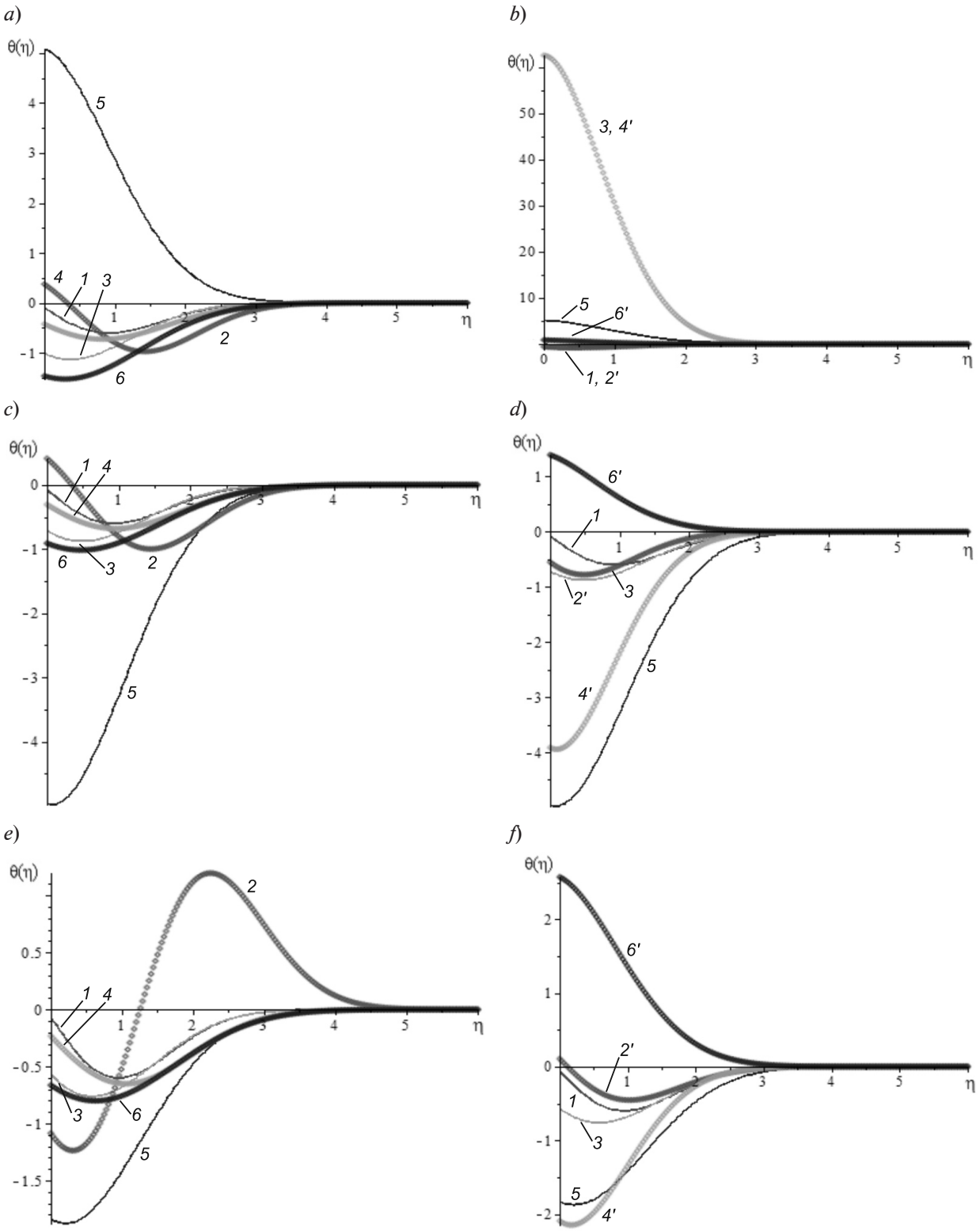

Fig. 6. Temperature profiles for flows of 3 nanofluid's compositions with various nanoparticle volume fractions ζ and three S values, in the presence of suction (*a*, *c*, *e*) and injection (*b*, *d*, *f*); there are (Cu − water) (*a*, *b*), (Al_2O_3 − water) (*c*, *d*) and (SWCNTs − water) (*e*, *f*) nanofluids; ζ = 0.01 (curves *1*, *2*, *2′*), 0.1 (*3*, *4*, *4′*), 0.2 (*5*, *6*, *6′*); S = 0.0 (*1*, *3*, *5*), 0.5 (*2*, *4*, *6*), −0.5 (*2′*, *4′*, *6′*)

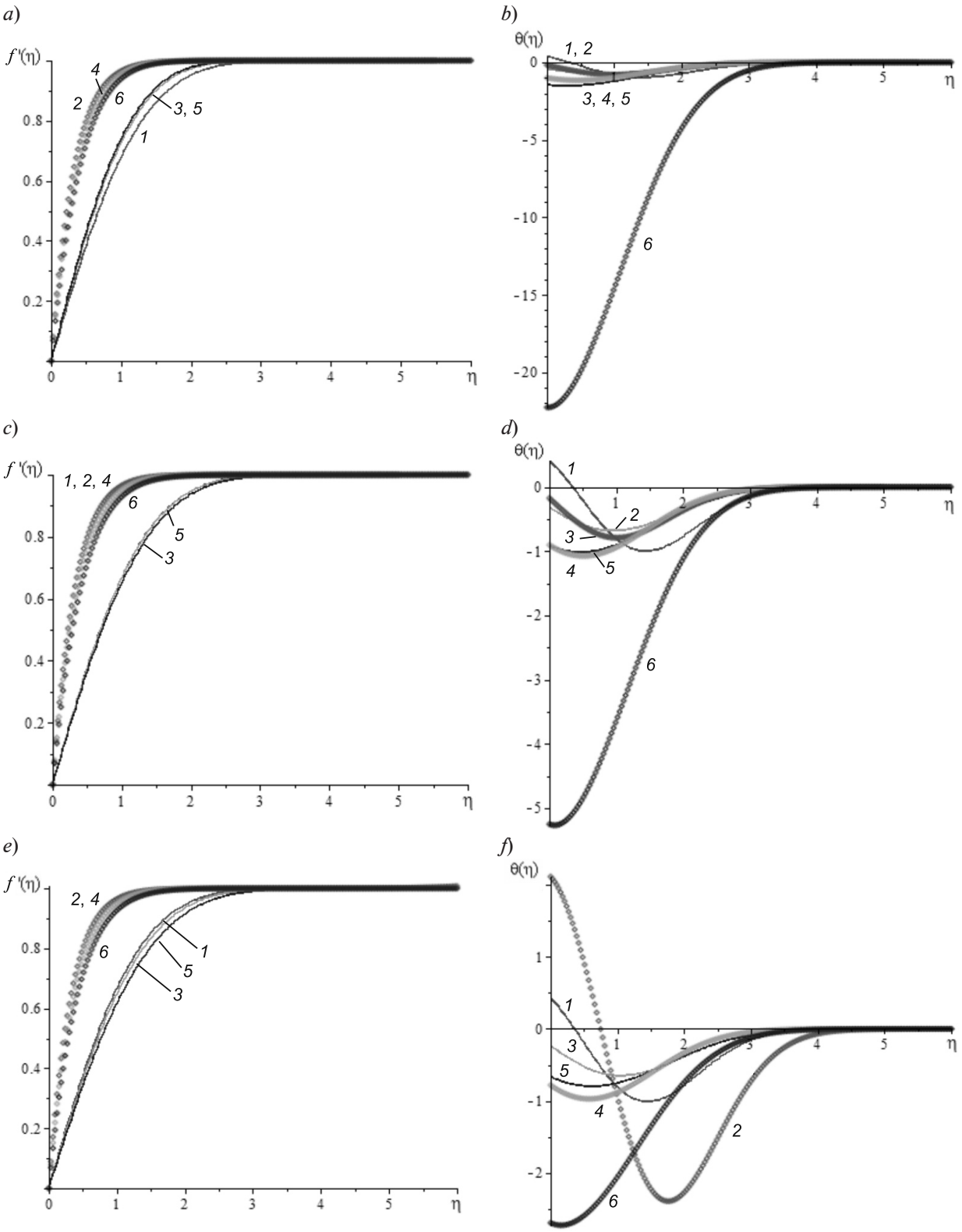

Fig. 7. Velocity (*a*, *c*, *e*) and temperature (*b*, *d*, *f*) profiles for flows of 3 nanofluid's compositions with various nanoparticle volume fractions ζ and two *M* values, in the presence of suction/injection; there are (Cu − water) (*a*, *b*), (Al_2O_3 − water) (*c*, *d*) and (SWCNTs − water) (*e*, *f*) nanofluids; ζ = 0.01 (curves *1*, *2*), 0.1 (*3*, *4*), 0.2 (*5*, *6*); *M* = 0.0 (*1*, *3*, *5*), 1.0 (*2*, *4*, *6*)

Table 5

Values of θ' (0) for various values of ζ and *S* obtained for different nanofluids

S	ζ	θ'(0)		
		Cu–water	Al_2O_3–water	SWCNTs–water
−0.5	0.01	−0.58606137	−0.55027344	0.1074283
	0.10	62.513571	−3.91577109	−2.09399467
	0.20	0.9053331	1.3937257	2.57353878
0.0	0.01	−0.09213680	−0.07197389	−0.06139028
	0.10	−1.01293273	−0.71568275	−0.56854083
	0.20	5.0843311	−4.96344745	−1.83299565
0.5	0.01	0.37498867	0.41074759	−1.08463332
	0.10	−0.42425009	−0.30778978	−0.23271640
	0.20	−1.46183727	−0.91021030	−0.66350571

Fixed parameter values: Pr = 6.2, $R = 0.5$, $b = 0.5$, $M = 1.0$, $\delta = 1.0$.

Table 6

Values of θ' (0) for various values of ζ and *M* obtained for different nanofluids

M	ζ	θ'(0)		
		Cu–water	Al_2O_3–water	SWCNTs–water
0.0	0.01	0.3749886	0.4107476	0.4298806
	0.10	−0.4242501	−0.3077898	−0.23271640
	0.20	−1.4618373	−0.9102103	−0.6635057
1.0	0.01	−0.1818800	−0.9028197	2.1186300
	0.10	−1.0052609	−0.7156827	−0.7817068
	0.20	−22.2641819	−5.2507555	−2.6988377

Fixed parameter values: Pr = 6.2, $R = 0.5$, $b = 0.5$, $S = 0.5$, $\delta = 1.0$.

Effect of ζ on temperature circulation of water-based Cu, Al_2O_3 and SWCNTs in the presence of heat source/sink is shown in Fig. 3. Heat source generates energy which causes the temperature of water-based Cu, Al_2O_3 and SWCNTs to first increase and then decrease in the boundary layer with increasing nanoparticle volume fraction, whereas the increasing nanoparticle volume fraction in the presence of the heat source parameter δ has the tendency to increase and decrease the thermal state in the boundary layer. The heat transfer rate of water-based Cu and SWCNTs first decreases and then increases with increasing nanoparticle volume fraction in the presence of heat source (see Table 3). It is interesting to note that the nanoparticle volume fraction of the water-based Cu plays a dominant role on the temperature field (in the presence of the heat source) compared with the other mixtures in squeezed flow regime. It can be seen from Fig. 4 that the temperature of water-based Al_2O_3 and SWCNTs decreases with increasing nanoparticle volume fraction in the presence of squeezed flow. The temperature of water-based Cu, Al_2O_3 and SWCNTs first decreases and then vibrates up and down with increasing nanoparticle volume fraction in the presence of thermal radiation (see Fig. 5). In the presence of thermal radiation, the heat transfer rate first increases and then decreases with increasing nanoparticle volume fraction (see Table 4). In the presence of suction, the temperature of water-based SWCNTs first increases and then

decreases with increasing nanoparticle volume fraction, whereas the opposite trend is observed for injection with increasing nanoparticle volume fraction (see Fig. 6). The nanoparticle volume fraction in the presence of suction has a significant effect on temperature field. In the presence of suction, it is also observed that the heat transfer rate of water-based SWCNTs first decreases and then increases with increasing nanoparticle volume fraction (see Table 5). For all three cases, it has been found that $f'(\eta)$ and $\theta(\eta)$ of the nanofluids decrease with increasing the nanoparticle volume fraction in the presence of a magnetic field. This is due to the combined effects of the Lorentz force with a size and a shape of the nanoparticle volume fraction (see Fig. 7 and Table 6), whereas the heat transfer rate increases with increasing the nanoparticle volume fraction when $M = 1.0$. In the presence of thermal radiation, heat generation and a magnetic field on the squeezed flow, it is observed that the temperature profiles for water-based SWCNTs are higher than those of other nanofluids, which implies that the SWCNTs show a unique combination of stiffness, energy, and inflexibility compared with other base materials which usually need one or more of these characteristics. Thermal and electrical conductivity of SWCNTs are also very high, and comparable to other conductive materials. An increase in the thermal boundary layer field due to an increase in the thermal conductivity shows that the temperature field increases gradually as we replace water-based copper by aluminum and SWCNTs in the sequence described in Figs. 3 – 7.

Conclusion

The performance of nanoparticle volume fraction of water-based Cu, Al_2O_3 and SWCNTs is examined between squeezing surfaces in such a form that the top plate is compressed. Association of temperature and the heat transfer rate among the nanofluids with different parameters are illustrated by figures and tables. The following conclusions can be drawn regarding the results obtained:

(*i*) In the presence of heat source/sink, the (Cu – water) nanofluid plays a dominant role in affecting the thermal boundary layer thickness with increasing the nanoparticle volume fraction compared with other mixtures in the squeezed flow region.

(*ii*) In the presence of squeezed parameter ($b = 1.0$) and at the nanoparticle volume fraction $\zeta = 0.2$, the temperature distribution of the (Cu – water) nanofluid attains its maximum, whereas the (Al_2O_3 – water) one attains its minimum value in the squeezed flow regime over a sensor surface.

(*iii*) In the presence of thermal radiation energy ($R = 1.0$), the temperature profiles of the (Cu – water) nanofluid increase and decrease with increasing the nanoparticle volume fraction as compared to the other mixtures in the squeezed flow regime.

(*iv*) In the presence of suction at the wall, the temperature distribution at the nanoparticle volume fraction $\zeta = 0.01$, in the presence of the (SWCNTs – water) nanofluid, attains its highest value compared with other mixtures in the squeezed flow regime over a sensor surface.

(*v*) In the presence of a magnetic field ($M = 10.0$), the (SWCNTs – water) nanofluid plays a dominant role with increasing the nanoparticle volume fraction due to its high thermal conductivity.

The thermal boundary layer thickness of the water-based SWCNTs are found to be much higher than those of other considered nanoparticles with the same volume fraction.

Being based on obtained results, we evaluated the efficiency of nanofluids as coolants in the laminar squeezed flow regimes. It was established that the water-based SWCNTs investigated in this paper can be beneficial in energy systems, rheology, material processing, lubrication and biomedical applications.

Appendix 1

List of symbols and units

B_0, $kg \cdot s^{-2} \cdot A^{-1}$, is the magnetic flux density;

c_p, $J \cdot kg^{-1} \cdot K^{-1}$, is the specific heat at constant pressure;

k^*, m^{-1}, is the mass absorption coefficient;

K, m^2, is the permeability of the porous medium;

k_f, $W \cdot m^{-1} \cdot K^{-1}$, is the thermal conductivity of the base fluid;

k_s, $W \cdot m^{-1} \cdot K^{-1}$, is the thermal conductivity of the nanoparticle;

k_{nf}, W·m^{-1}·K^{-1}, is the effective thermal conductivity of the nanofluid;

Pr is the Prandtl number;

M is the magnetic parameter;

q''_{rad}, kg·m^{-1}·s^{-3}·K^{-1}, is the incident radiation flux of intensity;

Q_0, kg·m^{-2}, is the rate of source/sink;

t, s, is the time;

T, K, is the temperature of the fluid;

T_w, K, is the temperature of the wall;

T_∞, K, is the temperature of the fluid far away from the wall;

R is the thermal radiation parameter;

u, v, m·s^{-1}, are the velocity components in x, y set;

$U(x)$, m·s^{-1}, is the velocity of the fluid away from the wedge;

V_0, m·s^{-1}, is the velocity of suction / injection;

α_{nf}, m^2·s^{-1}, is the nanofluid thermal diffusivity;

ρ_f, kg·m^{-3}, is the base fluid density;

ρ_s, kg·m^{-3}, is the nanoparticle density;

ρ_{nf}, kg·m^{-3}, is the nanofluid density;

$(\rho c_p)_{nf}$, J·m^{-3}·K^{-1}, is the heat capacitance of the nanofluid;

σ_{nf}, Ω^{-1}·m^{-1}, is the electric conductivity of the nanofluid;

σ_1, kg·s^{-3}·K^{-4} is the Stefan – Boltzman constant;

ν_f, m^2·s^{-1}, is the base fluid dynamic viscosity;

ν_{nf}, m^2·s^{-1}, is the nanofluid dynamic viscosity;

δ is the heat source / sink parameter;

λ is the porous parameter;

ζ is the nanoparticle volume fraction.

Appendix 2

I. Numerical solving

Eqs. (10), (11) subjected to boundary condition (12) are converted into the following simultaneous system of first order differential equations, as follows:

$$A_1 = (1-\zeta)^{2,5}\left(1-\zeta+\zeta\frac{\rho_s}{\rho_f}\right),$$
$$A_2 = (1-\zeta)^{2,5}\left(1-\zeta+\zeta\frac{\sigma_s}{\sigma_f}\right), \quad (15)$$
$$A_3 = 1-\zeta+\zeta\frac{(\rho c_p)_s}{(\rho c_p)_f}, A_4 = 1-\zeta,$$
$$A_5 = \frac{k_{nf}}{k_f A_3}+\frac{\Pr R}{k_f A_3};$$

$$f'(\eta) = u(\eta),\ u'f(\eta) = v(\eta),$$
$$v'(\eta) = -A_1\left(\left(f+\frac{b\eta}{2}\right)f'' - f'^2 + b(f'^2-1) + \right.$$
$$\left. + \left(M\frac{A_2}{A_1}+\frac{\lambda}{A_1}\right)(1-f')+1\right); \quad (16)$$
$$\theta'(\eta) = p(\eta),$$
$$p'(\eta) = -\frac{\Pr}{A_5}\left(\frac{\delta}{A_3}\theta+\left(f+\frac{b\eta}{2}\right)\theta' - \right.$$
$$\left. - \left(f'+\frac{b}{2}\right)\theta\right). \quad (17)$$

The boundary conditions are

$$f(0) = S, u(0) = 0, p(0) = -\frac{k_f}{k_{nf}};$$
$$u(L) = 1, \theta(L) = 0, v(0) = \alpha,\ \theta(0) = \beta, \quad (18)$$

where α, β are a priori unknowns to be determined as a part of the solution.

This software uses a fourth-fifth order Runge – Kutta – Fehlberg method with the shooting technique as a default to solve the boundary value problems numerically using the MAPLE 18 Dsolve command. The values of α and β are determined upon solving the boundary conditions

$$v(0) = \alpha, \theta(0) = \beta$$

on a trial and error basis.

The numerical results are represented in the form of the dimensionless velocity and temperature in the presence of water, ethylene glycol and engine oil-based SWCNTs, Cu and Al_2O_3.

II. Analytical solving using the optimal homotopy asymptotic method (OHAM)

On the OHAM grounds, the nonlinear ordinary differential equations (8) – (10) with boundary conditions (12) can be written as

$$f = f_0 + pf_1 + p^2 f_2,\ \theta = \theta_0 + p\theta_1 + p^2\theta_2;$$
$$H_1(p) = pC_1 + p^2C_2,\ H_2(p) = pC_3 + p^2C_4,$$

where $p \in [0,1]$ is the embedding parameter, H_p is the nonzero auxiliary function, C_i are constants [27].

III. Approximation of the momentum boundary layer problem

On the OHAM grounds, Eq. (10) and boundary conditions (12) can be written as

$$L = f'' + f',$$
$$N = f''' + A_1\left(\left(f + \frac{b\eta}{2}\right)f'' - f'^2 + b(f'^2 - 1) + \right.$$
$$\left. + \left(M\frac{A_2}{A_1} + \frac{\lambda}{A_1}\right)(1 - f') + 1\right) - f'' - f', \quad (19)$$

where L and N are the linear and the nonlinear operators, respectively.

After applying OHAM to Eq. (8) with respect to Eq. (12), we have

$$(1-p)[f'' + f'] =$$
$$= H_p\left[f''' + \left(A_1\left(f + \frac{b\eta}{2}\right)f'' - f'^2 + \right.\right.$$
$$\left.\left. + b(f'^2 - 1) + \left(M\frac{A_2}{A_1} + \frac{\lambda}{A_1}\right)(1 - f') + 1\right)\right], \quad (20)$$

and the zero-order equation p^0 of the boundary condition is

$$f_0'' + f_0' = 0,\ f_0(0) = S,\ \ f_0'(0) = 0. \quad (21)$$

The solution of the zero-order equation is

$$f_0(\zeta) = -[e^{-\zeta}(1 - e^{\zeta} + n - ne^{\zeta} -$$
$$- \alpha e^{\zeta} + \alpha n e^{\zeta})] / (1 + n). \quad (22)$$

The first-order equation p^1 is

$$f_1'' + f_1' = f_0'' + f_0' +$$
$$+ C_1\left[f_0''' + A_1\left(\left(f_0 + \frac{b\eta}{2}\right)f_0'' - f_0'^2\right) + \right.$$
$$\left. + b(f_0'^2 - 1) + \left(M\frac{A_2}{A_1} + \frac{\lambda}{A_1}\right)(1 - f_0') + 1\right]; \quad (23)$$
$$f_1(0) = 0,\ f_1'(0) = 0.$$

The second-order equation p^2 is

$$f_2'' + f_2' = f_1'' + f_1' +$$
$$+ C_1\left[f_1''' + A_1\left(\left(f_1 + \frac{b\eta}{2}\right)f_1'' - 2f_0'f_1' + \right.\right.$$
$$\left.\left. + 2bf_0'f_1' - 2f_0'f_1'\left(M\frac{A_2}{A_1} + \frac{\lambda}{A_1}\right)\right)\right] +$$
$$+ C_2\left[f_0''' + A_1\left(\left(f_0 + \frac{b\eta}{2}\right)f_0'' - f_0'^2 + \right.\right. \quad (24)$$
$$\left.\left. + b(f_0'^2 - 1) + \left(M\frac{A_2}{A_1} + \frac{\lambda}{A_1}\right)(1 - f_0') + 1\right)\right],$$
$$f_2(0) = 0,\ f_2'(0) = 0.$$

Solving Eqs. (23) and (24) with the boundary conditions using Eq. (22), the solution of Eq. (10) can be determined approximately in the following form:

$$f(\xi) = f_0(\xi) + f_1(\xi) + f_2(\xi). \quad (25)$$

Therefore, the residual equation takes the form

$$R_1(\xi, C_1, C_2) = \left[f'''(\xi) + A_1\left(\left(f(\xi) + \frac{b\xi}{2}\right)f''(\xi) - \right.\right.$$
$$-f'^2(\xi) + b(f'^2(\xi) - 1) + \quad (26)$$
$$\left.\left. + \left(M\frac{A_2}{A_1} + \frac{\lambda}{A_1}\right)(1 - f'(\xi)) + 1\right)\right].$$

The constants C_1 and C_2 can be optimally identified from the conditions

$$\frac{\partial J_1}{\partial C_1} = \frac{\partial J_1}{\partial C_2} = 0 \quad (27)$$

where $J_1(C_i) = \int_0^{\infty} R_1^2(\xi, C_i)\, d\xi$.

IV. Approximation of the energy boundary layer problem

On the OHAM grounds, Eq. (9) with the boundary condition (11) can be applied as

$$L = (\theta' + \theta),$$
$$N = \theta'' + \frac{\Pr}{A_5}\left(\frac{\delta}{A_3}\theta + \left(f + \frac{b\eta}{2}\right)\theta' - \right.$$
$$\left. - \left(f' + \frac{b}{2}\right)\theta\right) - (\theta' + \theta),$$

as before, L, N are the linear and the nonlinear operators.

Again, applying OHAM to Eq. (9) with respect to Eq. (11), we have

$$(1-p)[\theta' + \theta] = H_p\left[\theta'' + \frac{\mathrm{Pr}}{A_5}\left(\frac{\delta}{A_3}\theta + \left(f + \frac{b\eta}{2}\right)\theta' - \left(f' + \frac{b}{2}\right)\theta\right)\right]. \quad (28)$$

The zero-order equation p^0 is

$$(\theta_0^{'} + \theta_0) = 0,\ \theta_0(0) = 1. \quad (29)$$

Therefore the solution of Eq. (29) is

$$\theta_0(\xi) = e^{-\xi}. \quad (30)$$

The first-order equation p^1 is

$$\theta_1^{'} + \theta_1 = \theta_0^{'} + \theta_0 + C_3\left[\theta_0^{''} + \frac{\mathrm{Pr}}{A_5}\left(\frac{\delta}{A_3}\theta_0 + \left(f_0 + \frac{b\eta}{2}\right)\theta_0^{'} - \left(f_0^{'} + \frac{b}{2}\right)\theta_0\right)\right], \theta_1(0) = 0. \quad (31)$$

The second-order equation p^2 is

$$\theta_2^{'} + \theta_2 = \theta_1^{'} + \theta_1 + C_3\left[\theta_1^{''} + \frac{\mathrm{Pr}}{A_5}\left(\frac{\delta}{A_3}\theta_1 + \left(f_0 + \frac{b\eta}{2}\right)\theta_1^{'} + \left(f_1 + \frac{b}{2}\right)\theta_0^{'} - \left(f_0^{'} + \frac{b}{2}\right)\theta_1 - (f_1^{'})\theta_0\right) + C_4\left[\theta_0^{''} + \frac{\mathrm{Pr}}{A_5}\left(\frac{\delta}{A_3}\theta_0 + \left(f_0 + \frac{b\eta}{2}\right)\theta_0^{'} - \left(f_0^{'} + \frac{b}{2}\right)\theta_0\right)\right], \theta_2(0) = 0. \quad (32)$$

Solving Eqs. (31) and (32) with the boundary conditions with the help of Eq. (30), the solution of Eq. (11) can be determined approximately as

$$\theta(\xi) = \theta_0(\xi) + \theta_1(\xi) + \theta_2(\xi). \quad (33)$$

The residual equation takes the form

$$R_2(\xi, C_3, C_4) = \left[\theta''(\xi) + \frac{\mathrm{Pr}}{A_5}\left(\frac{\delta}{A_3}\theta(\xi) + \left(f(\xi) + \frac{b\xi}{2}\right)\theta'(\xi) - \left(f'(\xi) + \frac{b}{2}\right)\theta(\xi)\right)\right]. \quad (34)$$

The constants C_3, C_4 can be optimally derived from

$$\frac{\partial J_2}{\partial C_3} = \frac{\partial J_2}{\partial C_4} = 0 \quad (35)$$

where $J_2(C_i) = \int_0^\infty R_2^2(\xi, C_i)\, d\xi$.

The results obtained for $f''(0)$ in this work are compared with the solutions obtained in Ref. [32], for validation purposes (see Table 2).

REFERENCES

[1] **C. Xu, L. Yuan, Y. Xu, W. Hang,** Squeeze flow of interstitial Herschel-Bulkley fluid between two rigid spheres, Particuology. 8(4) (2010) 360–364.

[2] **Rizwan-ul-Haq, Z.H. Khan, S.T. Hussain, Z. Hammouch,** Flow and heat transfer analysis of water and ethylene glycol based Cu nanoparticles between two parallel disks with suction/injection effects, Journal of Molecular Liquids. 221 (2016) 298–304.

[3] **A.R.A. Khaled, K. Vafai,** Hydromagnetic squeezed flow and heat transfer over a sensor surface, Int. J. Eng. Sci. 42(5-6) (2004) 509–519.

[4] **M.M. Rashidi, H. Shahmohamadi, S. Dinarvand,** Analytic approximate solutions for unsteady two-dimensional and axisymmetric squeezing flows between parallel plates, Math. Probl. Eng. (2008) 935095.

[5] **A.M. Siddiqui, S. Irum, A.R. Ansari,** Unsteady squeezing flow of a viscous MHD fluid between parallel plates, a solution using the homotopy perturbation method, Math. Model. Anal. 13(4) (2008) 565–576.

[6] **F.N. Ibrahim, M. Terbeche,** Solutions of the laminar boundary layer equations for a conducting power law non-Newtonian fluid in a transverse magnetic field, J. Phys. D: Appl. Phys. 27(4) (1994) 740–747.

[7] **T. Watanabe, I. Pop,** Thermal boundary layers in magnetohydrodynamic flow over a flat plate in the presence of a transverse magnetic field, Acta Mech. 105(1-4) (1994) 233–238.

[8] **A.R.A. Khaled, K. Vafai,** Heat transfer and hydromagnetic control of flow exit conditions inside oscillatory squeezed thin films, Numer. Heat Transfer. Part A. 43(3) (2003) 239–258.

[9] **S.U.S. Choi,** Enhancing thermal conductivity of fluids with nanoparticles, International Mechanical Engineering Congress and Exposition San Francisco, USA, ASME. FED 231/MD. 66 (1995) 99–105.

[10] **N. Zhao, J. Yang, H. Li, Z. Zhang, S. Li,** Numerical investigations of laminar heat transfer and flow performance of Al_2O_3–water nanofluids in a flat tube, International Journal of Heat and Mass Transfer. 92 (2016) 268–282.

[11] **M.H. Aghabozorg, A. Rashidi, S. Mohammadi,** Experimental investigation of heat transfer enhancement of Fe_2O_3-CNT/water magnetic nanofluids under laminar, transient and turbulent flow inside a horizontal shell and tube heat exchanger, Experimental Thermal and Fluid Sci. 72 (2016) 182–189.

[12] **A. Aghanajafi, D. Toghraie, B. Mehmandoust,** Numerical simulation of laminar forced convection of water-CuO nanofluid inside a triangular duct, Physica E: Low-dimensional Systems and Nanostructures. 85 (2017) 103–108.

[13] **A.B. Rosmila, R. Kandasamy, I. Muhaimin,** Lie symmetry group transformation for MHD natural convection flow of nanofluid over linearly porous stretching sheet in presence of thermal stratification, Applied Mathematics and Mechanics (English Edition). 33(5) (2012) 593–604.

[14] **I. Muhaimin, R. Kandasamy, I. Hashim,** Thermophoresis and chemical reaction effects on non-Darcy MHD mixed convective heat and mass transfer past a porous wedge in the presence of variable stream condition,Chemical Engineering Research and Design. 87(11) (2009) 1527–1535.

[15] **R. Kandasamy, P.G. Palanimani,** Effects of chemical reactions, heat, and mass transfer on nonlinear magnetohydrodynamic boundary layer flow over a wedge with a porous medium in the presence of Ohmic heating and viscous dissipation, Journal of Porous Media. 10(10) (2007) 489–501.

[16] **R.U. Haq, S. Nadeem, Z.H. Khan, N.F.M. Noor,** Convective heat transfer in MHD slip flow over a stretching surface in the presence of carbon nanotubes, Phys. B: Condens. Matter. 457(2015) 40–47.

[17] **R. Ellahi, T. Hayat, F.M. Mahomed, A. Zeeshan,** Exact solutions of flows of an Oldroyd 8-constant fluid with nonlinear slip conditions, Z. Naturforschung A. 65(12) (2010) 1081–1086.

[18] **S. Nadeem, R.U. Haq, Z.H. Khan,** Numerical study of MHD boundary layer flow of a Maxwell fluid past a stretching sheet in the presence of nanoparticles, J. Taiwan Inst. Chem. Eng. 45 (1) (2014) 121–126.

[19] **R.E.M. Khan,** Exact solution for oscillatory rotating flows of a generalized Oldroyd-B fluid through porous medium, J. Porous Media. 12 (8) (2009) 777–788.

[20] **H. Masuda, A. Ebata, K. Teramae, N. Hishiunma,** Alteration of thermal conductivity and viscosity of liquid by dispersed ultra-fine particles (dispersion of Al_2O_3, SiO_2 and TiO_2 ultra-fine particles), Netsu Bussei (Japan). 7(4) (1993) 227–233.

[21] **S.U.S. Choi,** Enhancing Thermal Conductivity of Fluids with Nanoparticles, USA, ASME. FED 231/MD. 66 (1995) 99–105.

[22] **A. Karimipour, A. Taghipour, A. Malvandi,** Developing the laminar MHD forced convection flow of water/FMWNT carbon nanotubes in a microchannel imposed the uniform heat flux, Journal of Magnetism and Magnetic Materials. 419 (2016) 420–428.

[23] **A. Shahsavar, M. Saghafian, M.R. Salimpour, M.B. Shafii,** Experimental investigation on laminar forced convective heat transfer of ferrofluid loaded ith carbon nanotubes under constant and alternating magnetic fields, Experimental Thermal and Fluid Sci. 76 (2016) 1–11.

[24] **M. Nojoomizadeh, A. Karimipour,** The effects of porosity and permeability on fluid flow and heat transfer of multi walled carbon nano-tubes suspended in oil (MWCNT/Oil nano-fluid) in a microchannel filled with a porous medium, Physica E: Low-dimensional Systems and Nanostru. 84 (2016) 423–433.

[25] **A.D. Mansrah, U.A. Al-Mubaiyedh, T. Laui, et. al.,** Heat transfer enhancement of nanofluids using iron nanoparticles decorated carbon nanotubes, Applied Thermal Engg. 107 (2016) 1008–1018.

[26] **M. Imtiaz, T. Hayat, A. Alsaedi, B. Ahmad,** Convective flow of carbon nanotubes between rotating stretchable disks with thermal radiation effects, International Journal of Heat and Mass Transfer. 101 (2016) 948–957.

[27] **M.M. Rashidi, N. Freidoonimehr, A. Hosseini, O. Anwar Bég, T.-K. Hung,** Homotopy simulation of nanofluid dynamics from a nonlinearly stretching isothermal permeable sheet with transpiration, Meccanica. 49(2) (2014) 469–482.

[28] **A.R.A. Khaled, K. Vafai,** Hydromagnetic squeezed flow and heat transfer over a sensor surface, Int. J. Eng. Sci. 42(5-6) (2004) 509–519.

[29] **J.C. Maxwell,** A treatise on electricity and magnetism, 2nd edition, Clarendon Press, Oxford, UK (1881).

[30] **J.C. Maxwell,** A treatise on electricity and magnetism Oxford University Press, London, UK (1904) 435–441.

[31] **D. Pal and G. Mandal,** Influence of thermal radiation on mixed convection heat and mass transfer stagnation-point flow in nanofluids over stretching / shrinking sheet in a porous medium with chemical reaction, Nuclear Engineering and Design. 273 (2014) 644–652.

[32] **R.U. Hag, S. Nadeem, Z.H. Khan, N.F.M. Noor,** MHD squeezed flow of water functionalized metallic nanoparticles over a sensor surface, Physica E. 73 (2015) 45–53.

Received 01.06.2017, accepted 09.10.2017.

THE AUTHORS

KANDASAMY Ramasamy
Research Centre for Computational Mathematics, Tun Hussein Onn University of Malaysia, Parit Raja, Malaysia.
86400 Parit Raja, Batu Pahat, Johor, Malaysia
future990@gmail.com

ZAILANI Nanasha A.B.M.
Research Centre for Computational Mathematics, Tun Hussein Onn University of Malaysia, Parit Raja, Malaysia.
86400 Parit Raja, Batu Pahat, Johor, Malaysia
natashaazailani@yahoo.com

FATIHA Fatin N.B.J.
Research Centre for Computational Mathematics, Tun Hussein Onn University of Malaysia, Parit Raja, Malaysia.
86400 Parit Raja, Batu Pahat, Johor, Malaysia
fatinurfatiha93@gmail.com

СПИСОК ЛИТЕРАТУРЫ

1. **Xu C., Yuan L., Xu Y., Hang W.** Squeeze flow of interstitial Herschel-Bulkley fluid between two rigid spheres // Particuology. 2010. Vol. 8. No. 4. Pp. 360–364.

2. **Haq R.U., Khan Z.H., Hussain S.T., Hammouch Z.** Flow and heat transfer analysis of water and ethylene glycol based Cu nanoparticles between two parallel disks with suction/injection effects // Journal of Molecular Liquids. 2016. Vol. 221. Pp. 298–304.

3. **Khaled A.R.A., Vafai K.** Hydromagnetic squeezed flow and heat transfer over a sensor surface // Int. J. Eng. Sci. 2004. Vol. 42 No. 5–6. Pp. 509–519.

4. **Rashidi M.M., Shahmohamadi H., Dinarvand S.** Analytic approximate solutions for unsteady two-dimensional and axisymmetric squeezing flows between parallel plates // Math. Probl. Eng. 2008. No. 935095.

5. **Siddiqui A.M., Irum S., Ansari A.R.** Unsteady squeezing flow of a viscous MHD fluid between parallel plates, a solution using the homotopy perturbation method // Math. Model. Anal. 2008. Vol. 13. No. 4. Pp. 565–576.

6. **Ibrahim F.N., Terbeche M.** Solutions of the laminar boundary layer equations for a conducting power law non-Newtonian fluid in a transverse magnetic field // J. Phys. D: Appl. Phys. 1994. Vol. 27. No. 4. Pp. 740–747.

7. **Watanabe T., Pop I.** Thermal boundary layers in magnetohydrodynamic flow over a flat plate in the presence of a transverse magnetic field // Acta Mech. 1994. Vol. 105. No. 1–4. Pp. 233–238.

8. **Khaled A.R.A., Vafai K.** Heat transfer and hydromagnetic control of flow exit conditions inside oscillatory squeezed thin films // Numer. Heat Transfer. Part A. 2003. Vol. 43. No. 3. Pp. 239–258.

9. **Choi S.U.S.** Enhancing thermal conductivity of fluids with nanoparticles // International Mechanical Engineering Congress and Exposition San Francisco. USA. ASME. FED 231/MD. 1995. Vol. 66. Pp. 99–105.

10. **Zhao N., Yang J., Li H., Zhang Z., Li S.** Numerical investigations of laminar heat transfer and flow performance of Al_2O_3–water nanofluids in a flat tube // International Journal of Heat and Mass Transfer. 2016. Vol. 92. Pp. 268–282.

11. **Aghabozorg M.H., Rashidi A., Mohammadi S.** Experimental investigation of heat transfer enhancement of Fe_2O_3–CNT/water magnetic nanofluids under laminar, transient and turbulent flow inside a horizontal shell and tube heat exchanger // Experimental Thermal and Fluid Sci. 2016. Vol. 72. Pp. 182–189.

12. **Aghanajafi A., Toghraie D., Mehmandoust B.** Numerical simulation of laminar forced convection of water–CuO nanofluid inside a triangular duct // Phys. E. 2017. Vol. 85. Pp. 103–108.

13. **Rosmila A.B., Kandasamy R., Muhaimin I.** Lie symmetry group transformation for MHD natural convection flow of nanofluid over linearly porous stretching sheet in presence of thermal stratification // Applied Mathematics and Mechanics (Eng. Ed.). 2012. Vol. 33. No. 5. Pp. 593–604.

14. **Muhaimin I., Kandasamy R., Hashim I.** Thermophoresis and chemical reaction effects on non-Darcy MHD mixed convective heat and mass transfer past a porous wedge in the presence of variable stream condition // Chem. Eng. Res. and Des. 2009. Vol. 87. No. 11. Pp. 1527–1535.

15. **Kandasamy R., Palanimani P.G.** Effects of chemical reactions, heat, and mass transfer on nonlinear magnetohydrodynamic boundary layer flow over a wedge with a porous medium in the presence of Ohmic heating and viscous dissipation // Journal of Porous Media. 2007. Vol. 10. No. 5. Pp. 489–501.

16. **Haq R.U., Nadeem S., Khan Z.H., Noor N.F.M.** Convective heat transfer in MHD slip flow over a stretching surface in the presence of carbon nanotubes // Phys. B. 2015. Vol. 457. Pp. 40–47.

17. **Ellahi R., Hayat T., Mahomed F.M., Zeeshan A.** Exact solutions of flows of an Oldroyd 8 – constant fluid with nonlinear slip conditions // Z. Naturforschung A. 2010. Vol. 65. No. 12. Pp. 1081–1086.

18. **Nadeem S., Haq R.U., Khan Z.H.** Numerical study of MHD boundary layer flow of a Maxwell fluid past a stretching sheet in the presence of nanoparticles // J. Taiwan Inst. Chem. Eng. 2014. Vol. 45. No. 1. Pp. 121–126.

19. **Khan R.E.M.** Exact solution for oscillatory rotating flows of a generalized Oldroyd-B fluid through porous medium // J. Porous Media. 2009. Vol. 12. No. 8. Pp. 777–788.

20. **Masuda H., Ebata A., Teramae K., Hishiunma N.** Alteration of thermal conductivity and viscosity of liquid by dispersed ultrafine particles (dispersion of Al_2O_3, SiO_2 and TiO_2 ultrafine particles) // Netsu Bussei (Japan). 1993. Vol. 7. No. 4. Pp. 227–233.

21. **Choi S.U.S.** Enhancing thermal conductivity of fluids with nanoparticles // USA. ASME. FED 231/MD. 1995. Vol. 66. Pp. 99–105.

22. **Karimipour A., Taghipour A., Malvandi A.** Developing the laminar MHD forced convection flow of water/FMWNT carbon nanotubes in a microchannel imposed the uniform heat flux // Journal of Magnetism and Magnetic Materials. 2016. Vol. 419. Pp. 420–428.

23. **Shahsavar A., Saghafian M., Salimpour M.R., Shafii M.B.** Experimental investigation on laminar forced convective heat transfer of ferrofluid loaded with carbon nanotubes under constant and alternating magnetic fields // Experimental Thermal and Fluid Sci. 2016. Vol. 76. Pp. 1–11.

24. **Nojoomizadeh M., Karimipour A.** The effects of porosity and permeability on fluid flow and heat transfer of multi walled carbon nanotubes suspended in oil (MWCNT/Oil nanofluid) in a microchannel filled with a porous medium // Physica E. 2016. Vol. 84. Pp. 423–433.

25. **Mansrah A.D., Al-Mubaiyedh U.A., Laui T., et. al.** Heat transfer enhancement of nanofluids using iron nanoparticles decorated carbon nanotubes // Applied Thermal Eng. 2016. Vol. 107. Pp. 1008–1018.

26. **Imtiaz M., Hayat T., Alsaedi A., Ahmad B.,** Convective flow of carbon nanotubes between rotating stretchable disks with thermal radiation effects // International Journal of Heat and Mass Transfer. 2016. Vol. 101. Pp. 948–957.

27. **Rashidi M.M., Freidoonimehr N., Hosseini A., Anwar Bég O., Hung T.-K.** Homotopy simulation of nanofluid dynamics from a non-linearly stretching isothermal permeable sheet with transpiration // Meccanica. 2014. Vol. 49. No. 2. Pp. 469–482.

28. **Khaled A.R.A., Vafai K.,** Hydromagnetic squeezed flow and heat transfer over a sensor surface // Int. J. Eng. Sci. 2004. Vol. 42. No. 5–6. Pp. 509–519.

29. **Maxwell J.C.,** A Treatise on electricity and magnetism: 2nd edition. Oxford: Clarendon Press, 1881.

30. **Maxwell J.C.,** A Treatise on electricity and magnetism. London: Oxford University Press, 1904. Pp. 435–441.

31. **Pal D., Mandal G.** Influence of thermal radiation on mixed convection heat and mass transfer stagnation-point flow in nanofluids over stretching / shrinking sheet in a porous medium with chemical reaction // Nuclear Engineering and Design. 2014. Vol. 273. Pp. 644–652.

32. **Hag R.U., Nadeem S., Khan Z.H., Noor N.F.M.** MHD squeezed flow of water functionalized metallic nanoparticles over a sensor surface // Physica E. 2015. Vol. 73. Pp. 45–53.

Статья поступила в редакцию 01.06.2017, принята к публикации 09.10.2017.

СВЕДЕНИЯ ОБ АВТОРАХ

КАНДАСАМИ Рамасами – *сотрудник Исследовательского центра вычислительной математики Малайзийского университета Туна Хусейна Онна, г. Парит Раджа, Малайзия.*
86400 Parit Raja, Batu Pahat, Johor, Malaysia
future990@gmail.com

ЗАЙЛАНИ Наташа Амира Бинти Мод – *сотрудник Исследовательского центра вычислительной математики Малайзийского университета Туна Хусейна Онна, г. Парит Раджа, Малайзия.*
86400 Parit Raja, Batu Pahat, Johor, Malaysia
natashaazailani@yahoo.com

ФАТИХА Фатин Нур Бинти Джафар – *сотрудник Исследовательского центра вычислительной математики Малайзийского университета Туна Хусейна Онна, г. Парит Раджа, Малайзия.*
86400 Parit Raja, Batu Pahat, Johor, Malaysia
fatinurfatiha93@gmail.com